JACS
JOURNAL OF THE AMERICAN CHEMICAL SOCIETY

ARTICLE

pubs.acs.org/JACS

In Vivo Fluorescence Imaging of Bone-Resorbing Osteoclasts

Toshiyuki Kowada,[†] Junichi Kikuta,[‡,§] Atsuko Kubo,[‡,§] Masaru Ishii,[‡,§] Hiroki Maeda,[¶] Shin Mizukami,[†,¶] and Kazuya Kikuchi*[,†,¶]

[†]Laboratory of Chemical Imaging Techniques, Immunology Frontier Research Center (IFReC), Osaka University, Osaka, Japan
[‡]Laboratory of Cellular Dynamics, Immunology Frontier Research Center (IFReC), Osaka University, Osaka, Japan
[§]Japan Science and Technology Agency (JST), CREST, Tokyo, Japan
[¶]Department of Material and Life Science, Graduate School of Engineering, Osaka University, Osaka, Japan

Supporting Information

ABSTRACT: Osteoclasts are giant polykaryons responsible for bone resorption. Because an enhancement or loss of osteoclast function leads to bone diseases such as osteoporosis and osteopetrosis, real-time imaging of osteoclast activity in vivo can be of great help for the evaluation of drugs. Herein, pH-activatable chemical probes BAp-M and BAp-E have been developed for the detection of bone-resorbing osteoclasts in vivo. Their acid dissociation constants (pK_a) were determined as 4.5 and 6.2 by fluorometry in various pH solutions. These pK_a values should be appropriate to perform selective imaging of bone-resorbing osteoclasts, because synthesized probes cannot fluoresce intrinsically at physiological pH and the pH in the resorption pit is lowered to about 4.5. Furthermore, BAp-M and BAp-E have a bisphosphonate moiety that enabled the probes to localize on bone tissues. The hydroxyapatite (HA) binding assay in vitro was, therefore, performed to confirm the tight binding of the probes to the bone tissues. Our probes showed intense fluorescence at low pH values but no fluorescence signal under physiological pH conditions on HA. Finally, we applied the probes to in vivo imaging of osteoclasts by using intravital two-photon microscopy. As expected, the fluorescence signals of the probes were locally observed between the osteoclasts and bone tissues, that is, in resorption pits. These results indicate that our pH-activatable probes will prove to be a powerful tool for the selective detection of bone-resorbing osteoclasts in vivo, because this is the first instance where in vivo imaging has been conducted in a low-pH region created by bone-resorbing osteoclasts.

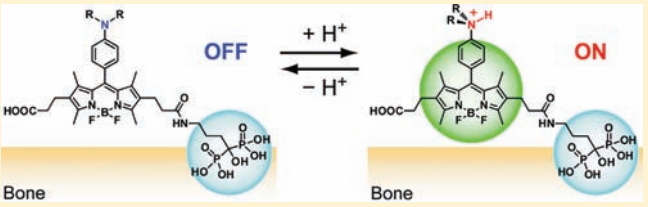

INTRODUCTION

Osteoclasts are giant multinucleated cells derived from monocytoid hematopoietic cells, which are responsible for bone resorption within the bone-remodeling compartment.[1−4] Because an enhancement or loss of osteoclast function causes bone diseases such as osteoporosis or osteopetrosis, real-time imaging of osteoclast activity in vivo is one of the most important tools required for investigations of osteoclast functions.[4] However, current bone imaging techniques such as computed tomography (CT) and biochemical markers of bone metabolism cannot connect spatial information with cellular activity. To overcome this problem, fluorescence imaging is a promising technique for obtaining temporal and spatial information about target cells or proteins.[5] Thus, we sought to develop fluorescent chemical probes with an OFF/ON switch, which can selectively detect active osteoclasts and thereby instantaneously provide an image of the location of the osteoclasts activated by particular stimuli. Furthermore, two-photon excitation microscopy can provide noninvasive imaging of osteoclasts in vivo.[6]

Active osteoclasts resorb the organic and inorganic components of the bone tissues by cathepsin K secretion and by proton extrusion, which causes acidification of the bone surface.[4] To the best of our knowledge, there have been no reports on the detection of protons extruded by osteoclasts. Only a single report has demonstrated the indirect in vivo detection of cathepsin K activity.[7] However, the cathepsin K probe has not yet provided real-time imaging data about the osteoclasts in the process of resorbing bone tissues, and its selectivity as a probe for the detection of osteoclast formation is inadequate.

We recognized that active osteoclasts can be selectively detected through specific imaging of low-pH regions by using a pH-activatable fluorescent probe[8] with specific delivery of the probe using a bisphosphonate group[9] (Figure 1a). In addition, this probe should be quite useful in the evaluation of drugs.

There are two requirements for the development of new probes for selective detection of bone-resorbing osteoclasts. One obvious requirement is a pH-sensitive fluorescence switch, and the other is the capability to localize on the bone tissue. Therefore, we designed fluorescent probes called "BAps". These probes are composed of boron−dipyrromethene (BODIPY) dye and a bisphosphonate group (Figure 1b). BODIPY dyes are

Received: July 12, 2011
Published: September 22, 2011

dx.doi.org/10.1021/ja2064582 | J. Am. Chem. Soc. 2011, 133, 17772–17776

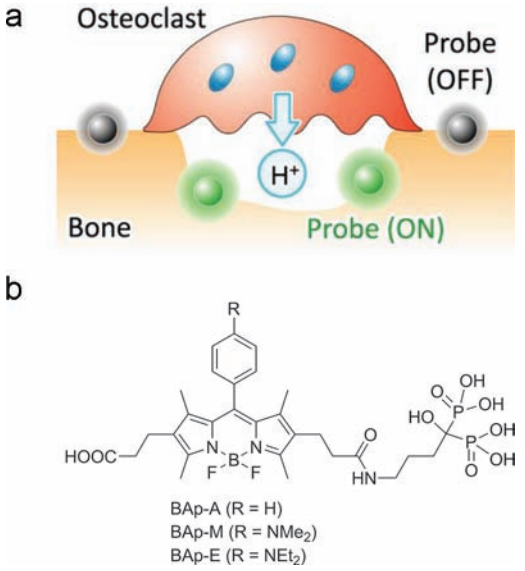

Figure 1. Strategy for selective detection of bone-resorbing osteoclasts using pH-activatable probes and design of BAps. (a) pH-activatable probes are immobilized on the bone tissue and provide intense fluorescence only when osteoclasts are resorbing bone. (b) Structures of the pH-activatable probes (BAps).

well-known fluorophores that have been used in a large number of applications because of their environmental stability, large molar absorption coefficients, and high fluorescence quantum yields.[10] Most recently, pH-activatable fluorescence probes including a BODIPY dye have been developed for the detection of cancers and real-time monitoring of therapy.[11] Furthermore, bisphosphonate compounds are currently used as drugs for the treatment of various bone diseases. These compounds chelate calcium and inhibit bone resorption. We, therefore, decided to combine a BODIPY-based pH-sensing unit with a bisphosphonate compound.

RESULTS AND DISCUSSION

Characterization of BAps. To demineralize the bone matrix, osteoclasts secrete protons (H^+) into the resorption pit where the pH value is lowered to about 4.5.[3] We, therefore, considered that selective imaging of osteoclasts would be achieved by the development of pH-activatable probes with an acid dissociation constant (pK_a) in the range of 4.5−6.5, because those probes cannot intrinsically fluoresce at the physiological pH. According to this assumption, we designed and synthesized three fluorescent probes with different pK_a values (Figure 1b). A control probe with "always-ON" fluorescence (BAp-A) was developed. The other probes are fluorescence "turn-ON" type sensors that can detect the acidic pH environment. Since the fluorescence OFF/ON switching mechanism is based on photoinduced electron transfer (PeT), the pK_a values of these probes can be finely tuned by the appropriate choice of an electron-donating moiety attached to the BODIPY core.[12] Thus, we chose *p*-dimethylanilino (BAp-M) and *p*-diethylanilino groups (BAp-E) as the electron-donating moieties to provide pK_a values in the range of 4.5−6.5.

The fluorescent probes were synthesized in one step from the corresponding dicarboxylic acids by using straightforward synthetic pathways (Scheme S1, Supporting Information). To confirm the pH-dependent fluorescence properties of BAps, we

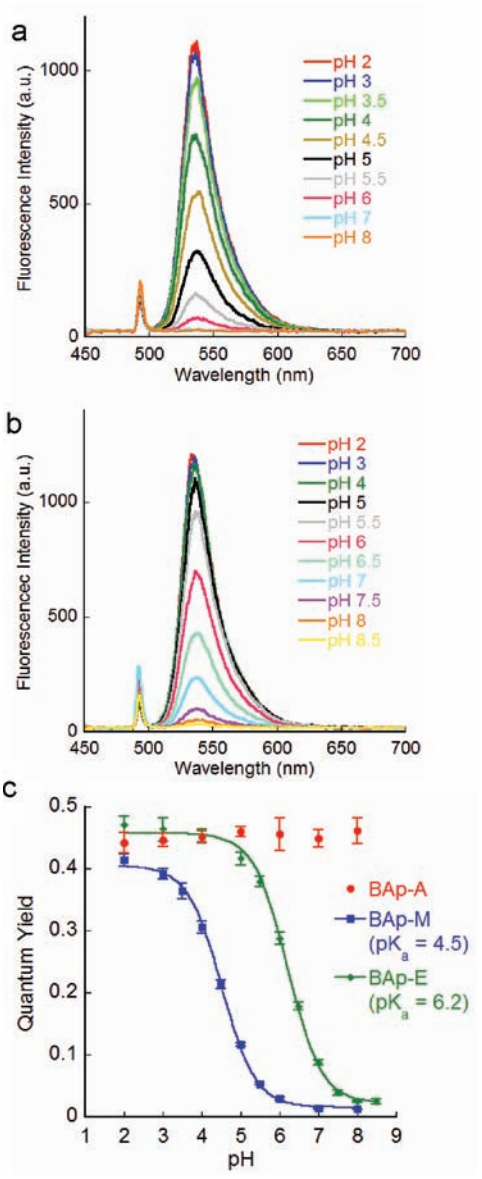

Figure 2. Fluorescence spectra (0.2 μM, excited at 492 nm) of (a) BAp-M and (b) BAp-E in citrate-phosphate buffer, and (c) pH-dependent profiles of changes in fluorescence quantum yield of BAps. The data were fitted to the Henderson−Hasselbalch equation.

measured the absorption and emission spectra in citrate-phosphate buffer at different pH values (Figures S1 and 2). All three probes had absorption maxima at about 520 nm. These peaks were found to be independent of the pH of the buffer. These results indicate that any structural changes or aggregations of the dye induced by pH changes do not occur in aqueous solution. In contrast, the fluorescence intensities of BAp-M and BAp-E were highly affected by the pH (Figure 2). The fluorescence intensities of BAp-M and BAp-E decreased along with an increase in pH. Essentially, no fluorescence was observed at the physiological pH. This phenomenon can be rationalized by the observation that PeT actually occurs from the *p*-anilino group to the BODIPY core.[12] Thus, these two probes showed a fluorescence "turn-ON" type increase at lower pH. Furthermore, the pK_a values were estimated by fitting pH-dependent changes of the fluorescence quantum yield to the

dx.doi.org/10.1021/ja2064582 |*J. Am. Chem. Soc.* 2011, 133, 17772–17776

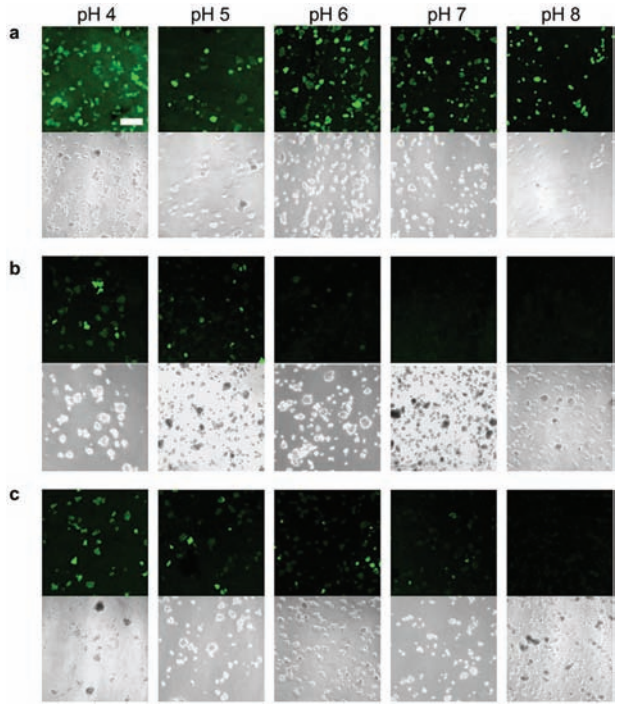

Figure 3. Confocal microscope images of BAps binding to hydroxyapatite in McIlvaine's citrate-phosphate buffer. Scale bar: 40 μm. (a) BAp-A. (b) BAp-M. (c) BAp-E.

Henderson−Hasselbalch equation (Figure 2c). Consequently, the pK_a values of BAp-M and BAp-E were 4.5 and 6.2, respectively. These results indicate that the two pH-activatable probes could be used to selectively visualize the bone-resorbing osteoclasts. On the other hand, BAp-A showed intense fluorescence regardless of pH changes as would be expected by an "always-ON" fluorescence probe.

Hydroxyapatite Binding Test. Bone tissues are mainly composed of type I collagen and hydroxyapatite (HA). Confocal microscopy was then performed to ascertain the HA binding activity and the fluorescence properties of BAps bound to HA. Intense fluorescence was observed from every HA particle, which was mixed with BAp-A and soaked in buffer at different pH values (Figure 3). We next examined the pH-activatable probes, namely, BAp-M and BAp-E. In the case of BAp-M, the fluorescence signals from HA particles were hardly observed under physiological conditions, i.e., at pH 7.0 and pH 8.0. The fluorescence intensities gradually increased with the decrease in the pH value, and consequently, intense fluorescence was observed below pH 5.0. Similar to the behavior in solution, the HA particle including BAp-E responded in an environment of higher pH relative to BAp-M, and showed intense fluorescence. However, the fluorescence signals were very weak or not observed at pH 7.0 or 8.0. These results indicate that BAps are pH-sensitive not only in aqueous solution but also in the solid state, when bound to HA. It was thus expected that synthesized probes could be immobilized on bone tissue and that they will retain their pH-sensitive properties in vivo.

In Vivo Imaging of Osteoclasts. To clarify the osteoclast function and develop new therapeutic agents to treat bone diseases, real-time monitoring of living osteoclasts in vivo will be very important. However, it is challenging to observe living osteoclasts that are present in the medullary cavity, deep inside the bone.

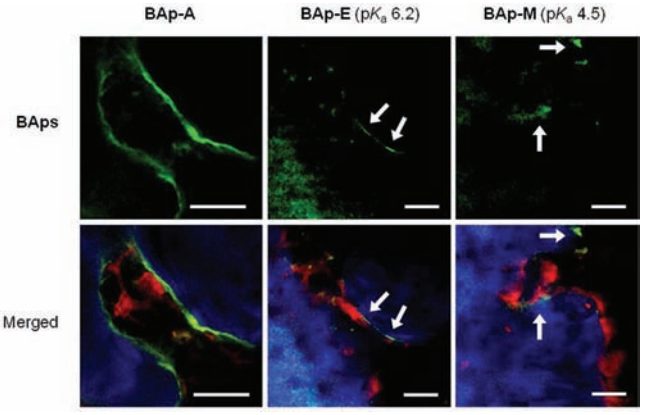

Figure 4. Two-photon excitation microscopy images of in vivo osteoclasts using BAps. PBS solution of BAps (green) was subcutaneously administered daily for 3 days to TRAP-tdTomato (red) transgenic mice. Second harmonic generation from collagen in the bone matrix is presented as a blue signal. Scale bars: 40 μm.

We used two-photon excitation microscopy, which can penetrate deeply into tissues, to capture images of osteoclasts through the parietal bone of mice.[6] The parietal bone is relatively thin, and the distance between the bone surface and the medullary cavity is 80−120 μm. This allowed us to achieve real-time imaging of the active osteoclasts in vivo. To ensure that BAps can function in a living mouse, we administered the probes to mice and evaluated their pH-sensitive properties by the above-described method (Figure 4). The blue signal indicates second harmonic generation from collagen fibers in the bone matrix. It is obvious that osteoclasts were present in the medullary cavity, because we used TRAP (tartrate-resistant acid phosphatase)-tdTomato transgenic mice, in which TRAP-positive mature osteoclasts predominantly express tdTomato.[13] To confirm whether the synthesized probes can be transported and immobilized on the bone tissues, we first used the "always-ON" probe BAp-A (Figure 4). As expected, green fluorescence was observed all over the bone surface. We next examined in vivo imaging of osteoclasts by using pH-activatable probes. In contrast to the case of BAp-A, green signals were locally observed only between the osteoclasts and the bone tissues (Figure 4, white arrow). Although the green staining was also observed in the lower left of the BAp-E panels, it is mainly derived from second harmonic generation from the bone matrix (Figure S2, Supporting Information). These results indicate that our probes are functioning properly, and have the potential to detect the bone-resorbing osteoclasts in vivo. Moreover, it is expected that the pH value in the resorption pit created by an osteoclast should be within the range of 4−6, because more intense fluorescence is found using BAp-E, which has a higher pK_a value relative to BAp-M. The brightness of BAp-E ($\varepsilon_{abs,450} \times \Phi$) between pH 4 and pH 6 is roughly 1.2−7.5 times as intense as that of BAp-M. Until now, the pH value in the resorption pit had not been measured in vivo. Therefore, we expect that this method will be helpful to estimate the pH value in the resorption pits.

■ CONCLUSION

We demonstrated that our custom-designed probes, in particular, BAp-E, fluoresce in the low-pH environment created by osteoclasts in vivo, as well as in a cuvette. From medicinal and

therapeutic points of view, an imaging technique for visualizing the migration and function of osteoclasts is highly desirable. Because this method is the first example of in vivo imaging of a low-pH region created by bone-resorbing osteoclasts, we are confident that the pH-activatable probes BAps will provide a powerful tool for the selective detection of bone-resorbing osteoclasts in vivo.

EXPERIMENTAL SECTION

Synthesis of BAp-A. To a solution of the corresponding bis-carboxylic acid (1,3,5,7-tetramethyl-2,6-bis(2-carboxyethyl)-8-phenyl-4,4-difluoro-4-bora-3a,4a-diaza-*s*-indacene)[11] (9.40 mg, 20.1 μmol) in MeCN (5 mL) were added alendronic acid (5.00 mg, 20.1 μmol) in water (4 mL), 2 N aq NaOH (60 μL, 120 μmol), and DMT-MM (27.7 mg, 100 μmol) at room temperature. After being stirred for 16 h, the reaction mixture was poured into 10% aqueous solution of AcOH (11 mL) and lyophilized. The crude compound was then purified by reverse-phase HPLC under the following conditions: A/B = 85/15 (0 min) to 10/90 (30 min) (solvent A: 100 mM aq TEAA; solvent B: acetonitrile). Compound eluted with a retention time of 12 min was collected. After lyophilization, a orange powder of BAp-A·3Et$_3$N was obtained (6.55 mg, 6.53 μmol) in 32% yield. ^{1}H NMR (400 MHz, D$_2$O) δ 0.95 (s, 3H), 0.97 (s, 3H), 1.12 (t, J = 7.2 Hz, 27H), 1.64−1.67 (m, 2H), 1.75−1.85 (m, 2H), 2.01−2.09 (m, 4H), 2.25−2.37 (m, 10H), 3.00−3.07 (m, 20H), 6.71 (br s, 2H), 7.14 (br s, 3H). HRMS (FAB−) Calcd for $[M - H^+]^-$ 698.2021, found 698.2010.

Synthesis of BAp-M. BAp-M was synthesized from the corresponding bis-carboxylic acid (1,3,5,7-tetramethyl-2,6-bis(2-carboxyethyl)-8-(*p*-dimethylaminophenyl-4,4-difluoro-4-bora-3a,4a-diaza-*s*-indacene)[11] by the same method as described above and purified by reverse-phase HPLC under the following conditions: A/B = 75/25 (0 min) to 60/40 (20 min), and then 10/90 (25 min) (solvent A: 100 mM aq TEAA; solvent B: acetonitrile). A orange powder of BAp-M·3Et$_3$N (t_R = 11 min) was obtained in 9% yield. ^{1}H NMR (400 MHz, D$_2$O) δ 1.10−1.14 (m, 33H), 1.63 (br s, 2H), 1.78 (br s, 2H), 2.02−2.10 (m, 4H), 2.28 (s, 3H), 2.32 (s, 3H), 2.41 (br s, 4H), 2.74 (s, 6H), 2.97−3.06 (m, 20H), 6.71 (br s, 4H). HRMS (FAB−) Calcd for $[M - H^+]^-$ 741.2443, found 741.2462.

Synthesis of BAp-E. BAp-E was synthesized from the corresponding bis-carboxylic acid (1,3,5,7-tetramethyl-2,6-bis(2-carboxyethyl)-8-(*p*-diethylaminophenyl-4,4-difluoro-4-bora-3a,4a-diaza-*s*-indacene)[11] by the same method as described above and purified by reverse-phase HPLC under the following conditions: A/B = 80/20 (0 min) to 10/90 (30 min) (solvent A: 100 mM aq TEAA; solvent B: acetonitrile). A orange powder of BAp-E·3Et$_3$N (t_R = 13 min) was obtained in 11% yield. ^{1}H NMR (400 MHz, D$_2$O) δ 0.95 (t, J = 7.2 Hz, 6H), 1.08 (s, 3H), 1.13 (t, J = 7.2 Hz, 27H), 1.18 (s, 3H), 1.60−1.65 (m, 2H), 1.71−1.83 (m, 2H), 2.03−2.11 (m, 4H), 2.28 (s, 3H), 2.35 (s, 3H), 2.40−2.46 (m, 4H), 2.93−2.98 (m, 2H), 3.05 (q, J = 7.2 Hz, 18H), 3.34 (q, J = 7.2 Hz, 4H), 6.93 (d, J = 8.0 Hz, 2H), 7.07 (d, J = 8.4 Hz, 2H). HRMS (FAB−) Calcd for $[M - H^+]^-$ 769.2756, found 769.2743.

High-Performance Liquid Chromatography. We performed HPLC on a system composed of a pump (PU-2080, JASCO) and a detector (MD-2010, JASCO) with an Inertsil ODS-3 (4.6 mm × 250 mm for analysis; 10.0 mm × 250 mm for preparation).

Fluorometry. Fluorescence spectra were measured in McIlvaine's citrate-phosphate buffer using a Hitachi F4500 spectrometer. Slit width was 2.5 nm for both excitation and emission, and the photomultiplier voltage was 950 V. Fluorescence quantum yields were determined using fluorescein in 0.1 N NaOH as a standard (Φ = 0.85, λ_{ex} = 492 nm).

In Vitro Hydroxyapatite Binding Test. Five milligrams/mL of hydroxyapatite was vortexed in a 1 μM aqueous solution of BAps (1 mL) for 30 min at room temperature. The mixture was centrifuged and washed four times with water. A portion of the residual powder was soaked in citrate-phosphate buffer (400 μL) at various pH values in a glass-bottom dish. Fluorescence images were then collected using a confocal laser scanning microscope (Olympus, FLUOVIEW FV10i) equipped with a 60× lens. The excitation wavelength was 473 nm, and the emission was filtered with a BA490−590 filter.

Two-Photon Excitation Imaging in Mice. The generation of TRAP promoter-tdTomato transgenic mice has been described elsewhere.[13] Twenty-five micrograms/body of BAp-A, BAp-E, or BAp-M dissolved in PBS was injected subcutaneously into TRAP-tdTomato mice once a day beginning 3 days prior to the recording of images. Intravital microscopy of mouse calvaria bone tissues was performed using a protocol modified from a previous study.[6] Mice were anesthetized with isoflurane (Escain; 2% vaporized in 100% oxygen), and the hair at the neck and scalp was removed with hair removal lotion (Kracie). The frontoparietal skull was exposed, and the mouse head was immobilized in a custom-designed stereotactic holder. The imaging system was composed of a multiphoton microscope (SP5; Leica) driven by a laser (Mai-Tai HP Ti: Sapphire; Spectraphysics) tuned to 900 nm and an upright microscope (DM6000B; Leica) equipped with a 20× water immersion objective (HCX APO, N.A. 1.0; Leica). The microscope was enclosed in an environmental chamber in which anesthetized mice were warmed by heated air. Fluorescent probes were detected through a bandpass emission filter at 525/50 nm. Osteoclasts were visualized by expression of TRAP-tdTomato (detected using a 585/40 nm filter). Snapshot images were acquired, and raw imaging data were processed with Imaris (Bitplane) with a Gaussian filter for noise reduction. In vivo imaging experiments were performed three times for each probe, and representative images are shown.

ASSOCIATED CONTENT

Supporting Information. Synthetic scheme, photophysical properties, and high-performance liquid chromatograms of BAps, and images of negative control experiment in vivo. This material is available free of charge via the Internet at http://pubs.acs.org.

AUTHOR INFORMATION

Corresponding Author
kkikuchi@mls.eng.osaka-u.ac.jp

ACKNOWLEDGMENT

This work was partially supported by the Japan Society for the Promotion of Science (JSPS) through its "Funding Program for World-Leading Innovative R&D on Science and Technology (FIRST) Program" and by the Ministry of Education, Culture, Sports, Science and Technology (MEXT) of Japan (Grant No. 22108519 and 20675004). K.K. and M.I. express their special thanks for support from the Takeda Science Foundation and the Mochida Memorial Foundation. K.K. also thanks the Naito Foundation for financial support. K.K. and S.M. acknowledge the Asahi Glass Foundation for financial support.

REFERENCES

(1) Boyle, W. J.; Simonet, W. S.; Lacey, D. L. *Nature* **2003**, *423*, 337–342.
(2) Raggatt, L. J.; Partridge, N. C. *J. Biol. Chem.* **2010**, *285*, 25103–25108.
(3) Teitelbaum, S. L. *Science* **2000**, *289*, 1504–1508.
(4) Rodan, G. A.; Martin, T. J. *Science* **2000**, *289*, 1508–1514.

(5) (a) Marks, K. M.; Nolan, G. P. *Nat. Methods* **2006**, *3*, 591–596. (b) Hinner, M. J.; Johnsson, K. *Curr. Opin. Biotechnol.* **2010**, *21*, 766–776. (c) Giepmans, B. N. G.; Adams, S. R.; Ellisman, M. H.; Tsien, R. Y. *Science* **2006**, *312*, 217–224. (d) Sadhu, K. K.; Mizukami, S.; Hori, Y.; Kikuchi, K. *ChemBioChem* **2011**, *12*, 1299–1308.

(6) Ishii, M.; Egen, J. G.; Klauschen, F.; Meier-Schellersheim, M.; Saeki, Y.; Vacher, J.; Proia, R. L.; Germain, R. N. *Nature* **2009**, *458*, 524–528.

(7) Kozloff, K. M.; Quinti, L.; Patntirapong, S.; Hauschka, P. V.; Tung, C.-H.; Weissleder, R.; Mahmoodet, U. *Bone* **2009**, *44*, 190–198.

(8) (a) Han, J.; Burgess, K. *Chem. Rev.* **2010**, *110*, 2709–2728. (b) Wang, R.; Yu, C.; Yu, F.; Chen, L. *Trends Anal. Chem.* **2010**, *29*, 1004–1013.

(9) (a) Roelofs, A. J.; Coxon, F. P.; Ebetino, F. H.; Lundy, M. W.; Henneman, Z. J.; Nancollas, G. H.; Sun, S.; Blazewska, K. M.; Bala, J. L. F.; Kashemirov, B. A.; Khalid, A. B.; McKenna, C. E.; Rogers, M. J. *J. Bone Miner. Res.* **2010**, *25*, 606–616. (b) Kashemirov, B. A.; Bala, J. L. F.; Chen, X.; Ebetino, F. H.; Xia, Z.; Russell, R. G. G.; Coxon, F. P.; Roelofs, A. J.; Rogers, M. J.; McKenna, C. E. *Bioconjugate Chem.* **2008**, *19*, 2308–2310. (c) Zaheer, A.; Lenkinski, R. E.; Mahmood, A.; Jones, A. G.; Cantley, L. C.; Frangioni, J. V. *Nat. Biotechnol.* **2001**, *19*, 1148–1154.

(10) (a) Loudet, A.; Burgess, K. *Chem. Rev.* **2007**, *107*, 4891–4932. (b) Ulrich, G.; Ziessel, R.; Harriman, A. *Angew. Chem., Int. Ed.* **2008**, *47*, 1184–1201.

(11) Urano, Y.; Asanuma, D.; Hama, Y.; Koyama, Y.; Barrett, T.; Kamiya, M.; Nagano, T.; Watanabe, T.; Hasegawa, A.; Choyke, P. L.; Kobayashi, H. *Nat. Med.* **2009**, *15*, 104–109.

(12) (a) Sunahara, H.; Urano, Y.; Kojima, K.; Nagano, T. *J. Am. Chem. Soc.* **2007**, *129*, 5597–5604. (b) Gabe, Y.; Urano, Y.; Kikuchi, K.; Kojima, H.; Nagano, T. *J. Am. Chem. Soc.* **2004**, *126*, 3357–3367.

(13) Kikuta, J.; Wada, Y.; Kowada, T.; Wang, Z.; Sun-Wada, G.-H.; Shimazu, Y.; Nishiyama, I.; Kubo, A.; Mizukami, S.; Maiya, N.; Yasuda, H.; Kikuchi, K.; Germain, R. N.; Ishii, M. Unpublished.